

# DESIGN STUDY OF THE DIPOLE MAGNET FOR THE RHIC EBIS HIGH ENERGY TRANSPORT LINE

Takeshi Kanesue, Kyushu University, Fukuoka 819-0395, Japan  
 Deepak Raparia, John Ritter, Masahiro Okamura, BNL, Upton, NY 11973  
 Jun Tamura, Tokyo Institute of Technology, Meguro-ku, Tokyo 152-8550, Japan

## Abstract

The design studies of the dipole magnet for EBIS HEBT line is proceeding. The RHIC EBIS is a new high current highly charged heavy ion preinjector for RHIC. The dipole magnet discussed in this paper will be used to guide the beam to existing heavy ion injection line to Booster. A total of 145 degrees bend is provided by two identical dipole magnets with a slit between these magnets to pass only intended charge state ions. Also this magnet has a hole in the side wall to pass the beam from the existing Tandem Van de Graaff. The performance of this magnet calculated by TOSCA and the results of the particle tracking calculation are described.

## INTRODUCTION

The RHIC EBIS will provide high current highly charged heavy ions from H to U for RHIC and NASA space Radiation Laboratory. RFQ and IH linac accelerate beams extracted from EBIS to 2 MeV / amu before HEBT dipole magnets. The layout of HEBT line is shown in Figure 1. Operation scheme requires the magnets to switch magnetic field corresponding to ion species within 1 second, and dipole magnet body should be laminated. In this paper, design methods of the dipole magnet to optimize magnetic field within required operating range is shown.

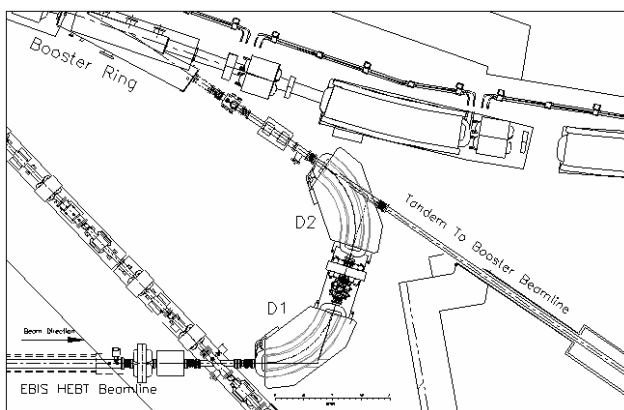


Figure 1: Layout of the EBIS HEBT dipole magnets

## MAGNET DESIGN

The bending section in EBIS HEBT line consists of two identical H type magnets with a slit between these magnets to eliminate unintended charge state ions. Each dipole magnet provides 72.5 degrees bend with 1.3 m bend radius and consequently total bend angle in this

section is 145 degrees. Gap height is 13.54 cm and required good field region is 5 cm centred on the beam axis. On the side wall of the magnet, there is a  $\phi 12.7$  cm hole to pass the beam from Tandem Van de Graafs. Magnet body is a laminated structure with up to 1mm thickness and the packing factor of the steel in the finished magnet will be 98% or better. Magnet dimension is limited because of limited space. Operation range is 0.157 - 0.964 T corresponding to  $H^+$  to  $Au^{32+}$ . Summary of magnet requirements are shown in Table. 1.

Table 1: requirements of the dipole magnet

gap height [cm]	13.54
operating range [T]	0.157-0.964
bend radius [m]	1.3
bend angle [degree]	72.5
useful aperture [cm]	5.0
hole radius on side wall[cm]	6.35

It is required to optimize dipole magnet design to minimize the difference of beam optics between low and high magnetic field. To achieve this performance, magnet design was completed with some steps. First, overall magnet dimension was decided to minimize iron surface saturation within 1.6 T within limited space. Then edge chamfer was modified not to change effective length of magnet within operation range. The effective length was defined as the length that integration of magnetic field ( $B_{total}$ ) along the reference orbit divided by  $B_{total}$  at the center of the magnet, here the reference orbit was defined as the ideal beam trajectory which had a 72.5 degrees bend angle and a 1.3 m bend radius and this reference orbit had enough length to include fringe field.

## CONDUCTOR

The upper and lower of the dipole will each have a 24 turn water-cooled main coil. The cross section of each main conductor is 22 mm x 22 mm. The 24 turn coil is made from three series electrically connected 8 turn pancake-type coils. Maximum current of main coil is 2250 A. The independently wired 24 turn trim coil shall be operated up to 2% of the primary coil magnetic maximum strength. The trim coil shall use solid conductor and shall be designed to be air-cooled or conduction cooled through the insulation to the main coil.

## SIMULATION

The design was simulated with OPEARA3D / TOSCA [1] using default iron BH curve as an iron property. A

conductor current corresponding to  $\text{He}^{2+}$  and  $\text{Au}^{32+}$  was used in the optimization process. The multipole components on the circle perpendicular to reference orbit with reference radius 5 cm were calculated for the vertical component of  $B_{\text{total}}$  ( $B_z$ ). The integral of the multipole components along the reference orbit was used to estimate dipole magnet performance. The integral of multipole components was expressed in the unit where 1 unit is corresponding to  $10^{-4}$  of the integral of main dipole components.

**EFFECT of HOLE**

At first, the effect of a hole on the side wall was estimated. The most affected region by the hole is clearly a close region to the hole. The effect was estimated on the perpendicular line to reference orbit toward the center of the hole. The difference of  $B_{\text{total}}$  on this line between a model with hole and a model without hole were calculated to evaluate local effect of the hole. The integral of multipole components along the reference orbit were also calculated to estimate effect to overall performance. These results are shown in Fig. 3 and table 2, respectively. In Fig. 3, horizontal axis is a distance from the reference orbit and vertical axis is the difference of  $B_{\text{total}}$ . Figure 3 and Table 2 show very small difference within useful aperture (50 mm). The difference of  $B_{\text{total}}$  on the line was less than 0.1 % and the difference of integral of multipole components was less than 0.2 %, respectively. Based on these results, we decided to use the 1 / 8 cutting model derived from geometrical symmetry to reduce a calculation time.

**LAMINATION**

Two kinds of lamination were compared to find the best packing method. The model 1 was packed to X direction of Fig. 4 and packing factor was 0.98 and the model 2 was packed to injection beam direction and had mirror image to the center of the magnet and packing factor was 0

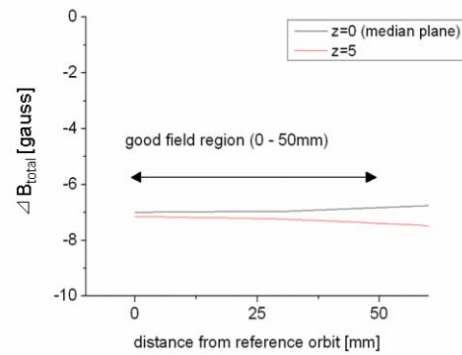


Figure 3: difference of  $B_{\text{total}}$  (hole model – nohole model) on the shortest line from reference orbit to center of the hole on side wall

Table 2: integral of multipole components on the reference radius 5 cm along the reference orbit. Quadrupole and sextupole components is expressed in  $10^{-4}$  units

	dipole [T*m]	quadrupole [unit]	sextupole [unit]
hole	1.61	10.46	-24.00
nohole	1.61	10.47	-24.02

contour about  $B_{\text{total}}$  in the high current case is shown in Fig4 (a), (b), where the contour is scaled from 0 to 1.6 T. The  $B_{\text{total}}$  on the transmitted region on the side wall is over 1.6 T where we call saturated region in this paper. Magnetic flux seemed to flow along the lamination, because saturated region was changed between two models where iron amount along the lamination was smaller compared to not-saturated region in each model.

Then we estimated the multipole components along the reference orbit. The quadrupole component was most affected and sextupole component is also discussed here. In low current simulation, quadrupole and sextupole

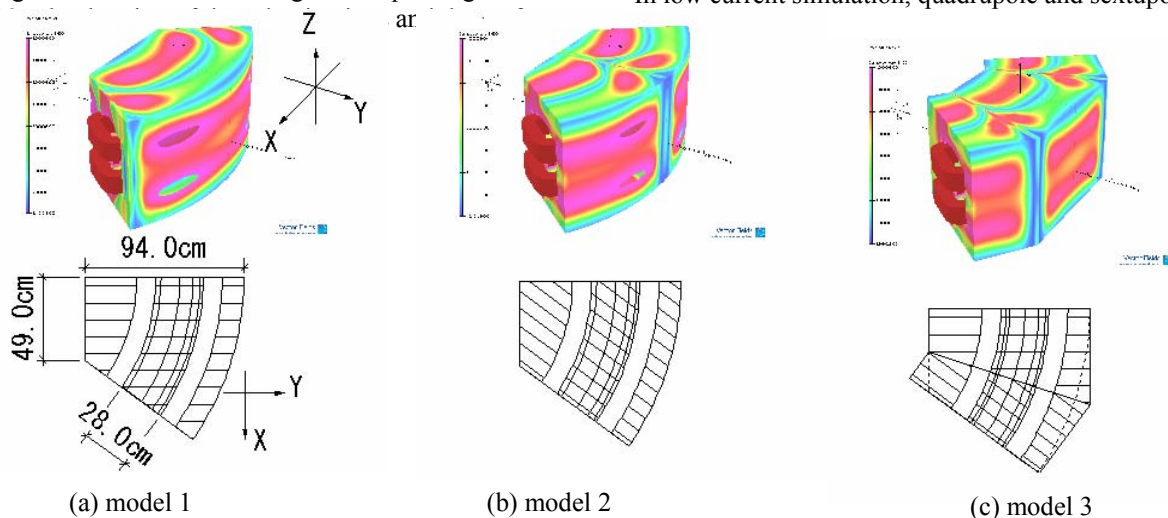


Figure 4: (a) model 1; packed in X direction, (b) model 2; packed in injection beam direction, (c) improved lamination derived from model 1 and model 2 where surface magnetic flux density does not exceed 1.5 T. All pictures has same scale from 0 to 1.6 T except for conductor. Conductor is red, its material color

component was also discussed here. In low current simulation, quadrupole and sextupole component has same shape between model 1 and 2, respectively, this is because magnet body was not saturated. In high current simulation, however, the components had difference at the saturated part between model 1 and model 2. The difference of the quadrupole component between model 1 and model 2 (shown in Fin. 5) is about 40 gauss and the difference of sextupole component is about 4 gauss. This difference can affect the beam optics between low and high current operation. In not saturated region, multipole component normalized by current density was well agreed between low and current simulation. This means that we might get same beam optics by reduction of saturation.

Based on these result, model 3 which has two lamination direction shown in Fig. 4. (c) was designed. The result of model 3 showed great performance that  $B_{total}$  on the surface became less than 1.5 T. Overall shape of multiple components normalized by current density had good similarity between low and high current (shown in Fig. 6), although here is a small difference at the lamination changing part that there was 6 gauss jump of quadrupole component and 2 gauss jump of sextupole

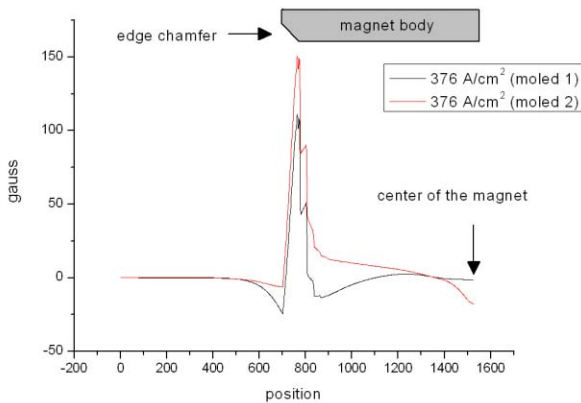


Figure 5: Quadrupole component of model 1 and model 2 along the reference orbit

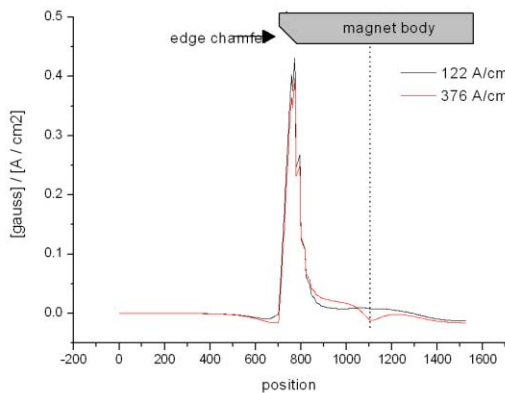


Figure 6: Quadrupole component of model 3 normalized by current density of conductor. lamination is changed at dotet line. Almost same field quality between low and high field case was achieved.

component. As shown above, magnet body part was optimized using combination of two types of lamination.

**EFFECTIVE LENGTH**

The effective length was optimized to achieve same effective length between the low and high field by optimizing edge chamfer cut with 45 degrees cutting angle. The 0x0 mm, 30x30 mm, 50x50 mm and 90x90 mm edge chamfer cut model was simulated. The result is shown in Fig. 6. Red plot is the effective length of low field, black plot is that of the high field. With the 90x 90 mm cutting, effective length deference between low and high field became less than 0.2 %.

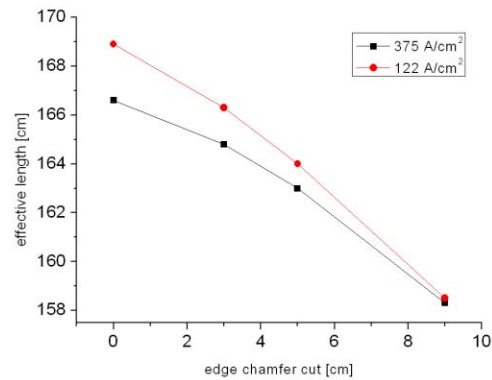


Figure 6: effective length change

**CONCLUSION**

The design study of dipole magnet for EBIS HEBT line was done after adding magnetic body to extend effective length to required length and optimizing shim shape to suppress the multipole components. The latest simulation result is shown in Table 3. Although some improvement is needed to reduce the sextupole component, this magnet design is almost satisfied the requirements. Through optimization process, we found that lamination direction can affect magnetic flux resulting saturation change. With this effect, also saturation can be controlled with combination of lamination direction. This effect could be effective for designing small magnet with big bend angle.

Table 3: integral of multipole component and effective length on latest model

Current density [A/cm <sup>2</sup> ]	dipole [T*m]	quadrupole [unit]	sextupole [Unit]	eff length [cm]
120	0.53	12.58	17.44	166.77
375	1.63	9.34	29.74	166.52

**REFERENCES**

[1] OPERA, Vector Fields Ltd, Oxford, UK